

# SOIL MANAGEMENT

## Identifying Soil Properties that Influence Cotton Yield Using Soil Sampling Directed by Apparent Soil Electrical Conductivity

D. L. Corwin,\* S. M. Lesch, P. J. Shouse, R. Soppe, and J. E. Ayars

### ABSTRACT

Crop yield inconsistently correlates with apparent soil electrical conductivity ( $EC_a$ ) because of the influence of soil properties (e.g., salinity, water content, texture, etc.) that may or may not influence yield within a particular field and because of a temporal component of yield variability that is poorly captured by a state variable such as  $EC_a$ . Nevertheless, in instances where yield correlates with  $EC_a$ , maps of  $EC_a$  are useful for devising soil sampling schemes to identify soil properties influencing yield within a field. A west side San Joaquin Valley field (32.4 ha) was used to demonstrate how spatial distributions of  $EC_a$  can guide a soil sample design to determine the soil properties influencing seed cotton (*Gossypium hirsutum* L.; 'MAXXA' variety) yield. Soil sample sites were selected with a statistical sample design utilizing spatial  $EC_a$  measurements. Statistical results are presented from correlation and regression analyses between cotton yield and the properties of pH, B,  $NO_3-N$ ,  $Cl^-$ , salinity, leaching fraction (LF), gravimetric water content, bulk density, percentage clay, and saturation percentage. Correlation coefficients of  $-0.01$ ,  $0.50$ ,  $-0.03$ ,  $0.25$ ,  $0.53$ ,  $-0.49$ ,  $0.42$ ,  $-0.29$ ,  $0.36$ , and  $0.38$ , respectively, were determined. A site-specific response model of cotton yield was developed based on ordinary least squares regression analysis and adjusted for spatial autocorrelation using maximum likelihood. The response model indicated that salinity, plant-available water, LF, and pH were the most significant soil properties influencing cotton yield at the study site. The correlations and response model provide valuable information for site-specific management.

**P**EDOGENIC AND ANTHROPOGENIC FACTORS result in soil variation within agricultural fields that affects crop productivity. A variety of physicochemical properties of soil influence crop production, including plant-available water; infiltration; permeability; soil texture and structure; soil depth; restrictive soil layers; organic matter; chemical constituents such as salinity, fertilizers, pesticides, trace elements, and toxic ions; meteorology; and landscape features such as microelevation and topography (Black, 1968; Thornley and Johnson, 1990; Hanks and Ritchie, 1991; Tanji, 1996). In laser-leveled, irrigated agricultural lands of the arid southwestern USA, soil physicochemical properties such as salinity, soil texture and structure, plant-available water, trace elements (particularly B), and ion toxicity ( $Na^+$  and  $Cl^-$ ) are the primary soil factors influencing crop yield (Tanji, 1996). These properties tend to be highly spatially variable. Site-specific crop management (or precision agriculture) has been proposed as a means of coping with spa-

tially variable soil properties that affect crop yield to better optimize crop productivity and to maintain the sustainability of agriculture.

Site-specific crop management is the management of soils, pests, and crops based on spatial variations within a field (Larson and Robert, 1991). Site-specific management utilizes rapidly evolving electronic information technologies to modify land management in a site-specific manner as conditions change spatially and temporally (van Schilfhaarde, 1999). The aim of precision agriculture is to improve management to increase profitability, increase crop productivity, sustain the soil-plant-water environment, and/or reduce detrimental environmental impacts (Atherton et al., 1999).

Precision agriculture is a technologically driven system (van Schilfhaarde, 1999). First conceived in the mid 1980s, the technological pieces needed to bring precision agriculture into its own began to fall into place in the mid 1990s with the maturation of global positioning systems (GPS) and geographical information systems (GIS). These and other new technologies potentially provide the ability to (i) quantify yield variability in small areas of the field; (ii) quantify the spatial variability of soil properties influencing yield; and (iii) adjust inputs such as fertilizer, pesticide, and seeding rates based on knowledge of soil and yield variability (Atherton et al., 1999). The measurement of  $EC_a$  is among the technologies that are helping to bring precision agriculture from a concept to a tool for addressing the issue of agricultural sustainability.

Bullock and Bullock (2000) point out that efficient methods for accurately measuring within-field variations in soil physical and chemical properties are important for precision agriculture. Soil  $EC_a$  has become one of the most reliable and frequently used measurements to characterize field variability for application to precision agriculture due to its ease of measurement and reliability (Rhoades et al., 1999a, 1999b; Corwin and Lesch, 2003). For instance, it has been previously shown by Kitchen et al. (1999) using boundary-line analysis that soil  $EC_a$  provides a measure of the within-field soil differences associated with topsoil thickness, which for claypan soils, is a measure of root zone suitability for crop growth and yield. The potential of the spatial measurement of profile  $EC_a$  for predicting crop yield due to soil differences has been reported by Jaynes et al. (1995) and Sudduth et al. (1995). The rapid spatial mea-

D.L. Corwin, S.M. Lesch, P.J. Shouse, USDA-ARS, George E. Brown, Jr., Salinity Lab., 450 West Big Springs Rd., Riverside, CA 92507-4617; and R. Soppe and J.E. Ayars, USDA-ARS, Water Manage. Res. Lab., 9611 S. Riverbend Ave., Parlier, CA 92648. Received 22 Mar. 2002. \*Corresponding author (dcorwin@ussl.ars.usda.gov).

**Abbreviations:**  $EC_a$ , apparent soil electrical conductivity;  $EC_e$ , electrical conductivity of the saturation extract; GIS, geographical information systems; GPS, global positioning systems; LF, leaching fraction; OLS, ordinary least squares; SP, saturation percentage;  $\theta_v$ , gravimetric water content;  $\rho_b$ , bulk density.

Published in Agron. J. 95:352-364 (2003).

surement of soil  $EC_e$  has been demonstrated using both mobile electromagnetic (EM) induction (McNeil, 1992; Rhoades, 1992a, 1992b; Carter et al., 1993; Jaynes et al., 1993; Kitchen et al., 1996) and mobile electrical resistivity equipment (Rhoades, 1992a, 1992b; Carter et al., 1993).

Precision agriculture studies relating crop yield directly to  $EC_e$  have met with inconsistent results due to the complex interaction of soil properties that influence the  $EC_e$  measurement, thereby confounding results (Corwin and Lesch, 2003). These soil properties include soil salinity, clay content and cation exchange capacity, clay mineralogy, soil pore size and distribution, soil moisture content, organic matter, bulk density ( $\rho_b$ ), and soil temperature (McNeil, 1992; Rhoades et al., 1999a, 1999b; Corwin and Lesch, 2003).

In instances where yield correlates with  $EC_e$ , spatial measurements of  $EC_e$  can be used in a precision agriculture context (Corwin and Lesch, 2003). More specifically, spatial  $EC_e$  information can be used to develop a directed soil sampling plan that identifies sites adequately reflecting the range and variability of various soil properties thought to influence crop yield. This is advantageous because the cost of obtaining soil samples to characterize field spatial variability is a key problem in precision agriculture.

Cotton yield in California's San Joaquin Valley is thought to be influenced by a variety of soil physical and chemical properties including, but not limited to, salinity [electrical conductivity of the saturation extract ( $EC_e$ )], texture,  $\rho_b$ , LF, B,  $NO_3-N$ , and plant-available water. Similarly, the  $EC_e$  measurement of high clay content soils of the arid San Joaquin Valley is influenced by the properties of  $EC_e$ , texture, water content, and  $\rho_b$  and often correlates with soil B levels and LF (Rhoades et al., 1999a, 1999b; Corwin and Lesch, 2003; Corwin et al., 2003). It is hypothesized that in instances where cotton yield correlates with  $EC_e$ , the spatial distribution of  $EC_e$  could provide a means of determining the effects of soil variability on yield by guiding an optimized sample design of soil properties influencing yield.

The objectives of this study were to (i) determine the correlation between cotton yield and  $EC_e$  for a site in the San Joaquin Valley; (ii) utilize an intensive spatial survey of  $EC_e$  to devise a soil sampling scheme that will identify soil properties influencing cotton yield; (iii) correlate cotton yield with spatially associated soil physicochemical properties, including gravimetric water content ( $\theta_g$ ),  $EC_e$ , B, pH, percentage clay,  $\rho_b$ ,  $NO_3-N$ ,  $Cl^-$ , LF, and saturation percentage (SP); and (iv) develop a site-specific cotton yield response model.

## METHODS AND MATERIALS

### Study Site Description

The study site was a 32.4-ha field (west half of quarter section 4-2) located in the Broadview Water District on the west side of the San Joaquin Valley in central California (Fig. 1). The 4000-ha Broadview Water District is located in the northwest corner of Fresno County. The field was planted with cotton. The soil at the study site is a Panoche silty clay (thermic Xerorthents), which is slightly alkaline and has good surface and subsurface drainage (Harradine, 1950). The sur-



Fig. 1. Map showing the location of the Broadview Water District in California's Fresno County, which lies in the San Joaquin Valley.

face of the Panoche series is light brownish gray, light yellowish brown, or pale brown; calcareous; and widely variable in texture. It is thick and friable and easily penetrated by roots and water. Where the soil is moderately fine textured, it becomes sticky when wet but is easily worked when dry. The subsoil, to a depth of 1.8 m, is very similar to the surface soil. There may be an increase of lime content in a segregated form or small quantities of gypsum, but there is no definite development of structural units. The parent material is sedimentary alluvium.

### Cotton Yield Monitoring and Data

Spatial distributions of cotton yield were measured with a four-row cotton picker equipped with a yield sensor and GPS. The GPS unit used was an AG132. Yield sensors used a light source and an eye through two of the four chutes on a cotton picker to measure average seed cotton yield (conversion: seed cotton  $\times$  0.34 = lint cotton). All subsequent referrals to cotton yield are with respect to seed cotton yield. The GPS receiver accuracy was to within 1 m of horizontal accuracy. The spatial cotton yield data were collected during the August 1999 harvest. It was not clear from the original 10 000+ raw cotton yield measurements what constituted a reasonable lower bound for legitimate readings, so an arbitrary value of 1 Mg ha<sup>-1</sup> was chosen as the cutoff. This eliminated nearly all near-zero readings that were due to field-edge effects and the presence of a temporary unlined irrigation canal that had been excavated in an east-west direction through the middle of the field and then filled in before the yield monitoring. The raw data set was reduced to 7706 clean cotton yield readings. Each yield observation represented a total area of approximately 42 m<sup>2</sup>. From the time of the previous harvest in August 1999 until planting in April 2000, the field was fallow.

### Intensive Fixed-Array Apparent Soil Electrical Conductivity Survey

The methods and materials that were used in this study for conducting an  $EC_e$  survey followed the suggested guidelines of Corwin and Lesch (2003). Mobile fixed-array electrical resistivity equipment developed by Rhoades and colleagues (Rhoades, 1992a, 1992b; Carter et al., 1993) was used in an intensive  $EC_e$  survey. The intensive  $EC_e$  survey was conducted in March 2000 following a preplant irrigation to bring the

study site to field capacity. The fixed-array electrodes were set to measure  $EC_a$  to a depth of roughly 1.2 to 1.5 m. Approximately 4000+  $EC_a$  measurements were taken across the 32.4-ha study area. Each  $EC_a$  measurement was georeferenced using GPS.

### Soil Sampling Design

Once the intensive  $EC_a$  survey was conducted, the ESAP-95 version 2.01 software package developed by Lesch et al. (1995a, 1995b, 2000) was used to establish the locations where soil cores were taken based on the  $EC_a$  survey data. Using a model-based sampling strategy, 60 sites were selected that reflected the observed spatial variability in  $EC_a$  while simultaneously maximizing the spatial uniformity of the sampling design across the study area. The number of sites is user-defined in ESAP. In this particular instance, 60 sites (six depths at each site) were selected as the maximum number of samples that could be analyzed with the available resources to characterize any encountered spatial autocorrelation. A detailed discussion of the application of a model-based sampling strategy using  $EC_a$  survey data can be found in Lesch et al. (1995b). Figure 2 is a map of the 4000+  $EC_a$  measurements and the 60 locations selected with the ESAP software.

Soil cores were taken at the 60 sites with a Giddings rig at 0.3-m increments to a depth of 1.8 m. Two sets of cores were taken for each depth increment. The duplicate cores were taken within 7.5 to 10 cm of one another. One set of soil cores was taken for  $\rho_b$  determination (Blake and Hartge, 1986), and another set was taken for soil chemical and physical property analysis. All samples were bagged in zip-lock bags and stored in an ice chest until they could be refrigerated. At 17 locations, soil cores could not be taken at the deepest depth increment (i.e., 1.5–1.8 m) because the water table had been reached and the sample was saturated, causing it to run out of the core tube before reaching the soil surface. This resulted in two sets of 343 soil samples.

## $EC_a$ Survey & Soil Core Sites

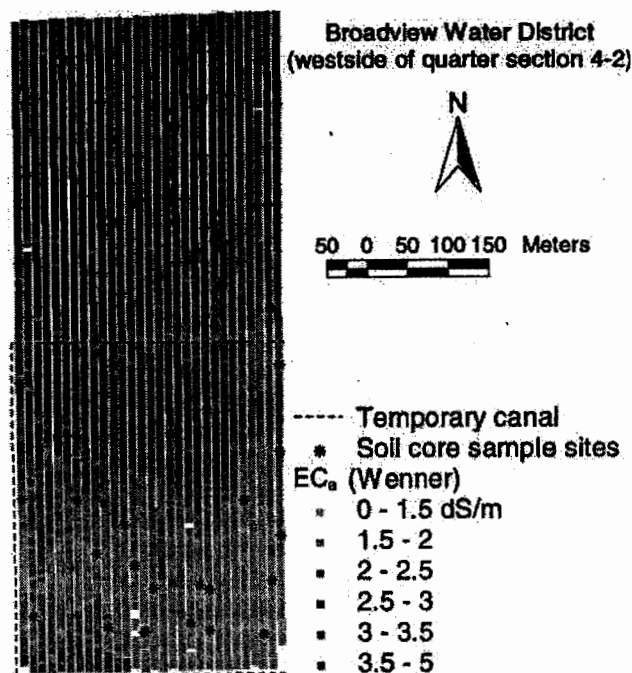


Fig. 2. Map of the intensive apparent soil electrical conductivity ( $EC_a$ ) survey and the 60 soil-core sites. Positions of the soil-core sites are indicated with an asterisk (\*). Dashed line indicates the temporary flood irrigation canal.

## Soil Chemical and Physical Analyses

In the field, a subsample (200–400 g) of each core from the set of samples designated for chemical and physical property analysis was taken for soil moisture content determination. The subsamples were weighed in the field to minimize any error due to moisture loss. These subsamples were later oven-dried at 110°C for 24 h and weighed again to determine  $\theta_s$ .

The 343 soil samples designated for analysis of soil chemical and physical properties were analyzed for pH, B,  $NO_3-N$ ,  $Cl^-$ , EC, and percentage clay. Solution extracts were taken from 1:1 soil/water mixtures. The 1:1 extracts were analyzed for pH,  $NO_3-N$ ,  $Cl^-$ , EC, and B following procedures outlined in Agronomy Monograph No. 9 (Page et al., 1982). From the electrical conductivity from the 1:1 extracts and from the SP,  $EC_e$  was calculated because  $EC_e$  is the most common representation of soil salinity. The second set of 343 soil samples was used to determine  $\rho_b$ . The LF was estimated by dividing the average  $Cl^-$  concentration of the irrigation water by the  $Cl^-$  concentration of the saturation extract at the 1.2- to 1.5-m depth increment. The  $Cl^-$  concentration of the saturation extract at the 1.2- to 1.5-m depth increment was used because 0 to 1.5 m was selected as the root zone of cotton at the study site. The rationale for using the 0 to 1.5 m as the root zone is discussed in the following section. Particle size distribution was measured using the hydrometer method (Gee and Bauder, 1986).

## Simple Statistical Correlations and Cotton Yield Modeling

For all statistical correlation and regression analyses, the average over the root zone (0–1.5 m) at each site was used. Simple correlations were determined between yield and the physicochemical properties of  $\theta_s$ ,  $EC_e$ , B, pH, percentage clay,  $\rho_b$ ,  $NO_3-N$ ,  $Cl^-$ , LF, and SP. Correlations between the physicochemical properties and  $EC_e$  and between cotton yield and  $EC_e$  were also determined.

The cotton yield data collected during the study did not exactly overlap with the  $EC_e$  survey data; consequently, ordinary kriging was used to determine the expected cotton yield at the 60 soil-core sites. The spatial correlation structure of yield was modeled with an isotropic variogram (Fig. 3). As shown in Fig. 3, the overall structure revealed a sizable nugget term, suggesting the existence of considerable localized yield variation most likely due to large measurement error caused by yield-monitoring dynamics. The following exponential variogram model was used to describe this spatial structure:

## Semivariogram of Cotton Yield

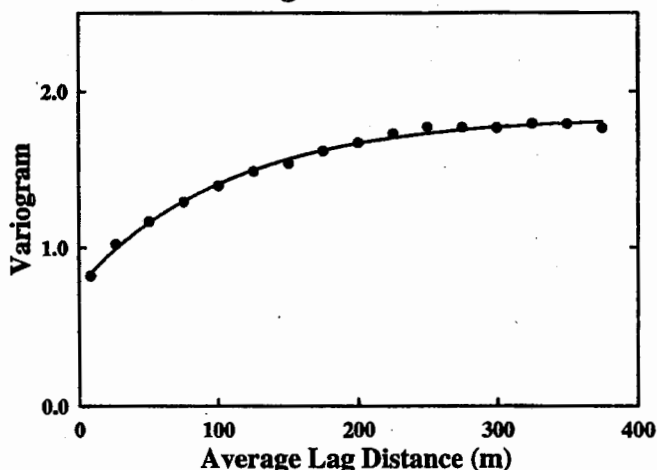


Fig. 3. Calculated semivariogram of cotton yield. The points are the experimental variogram for all 7706 points while the solid line represents the fitted variogram.

$$v(\delta) = \eta^2 + \sigma^2[1 - \exp(-D/\alpha)] \quad [1]$$

where  $\eta^2$  represents the nugget variance,  $\sigma^2$  the spatial variance component (partial sill),  $D$  the lag distance, and  $\alpha$  the range parameter. A nonlinear least-squares fitting algorithm was used to estimate the three variogram model parameters (standard errors are in parentheses):  $\eta^2 = 0.76$  (0.02),  $\sigma^2 = 1.08$  (0.02), and  $\alpha = 109.3$  (5.97). This fitted variogram model was then used in an ordinary kriging procedure to estimate the expected yield at the 60 sample sites. The mean estimated yield for the sample sites was 5.95 Mg ha<sup>-1</sup>, with a range from 3.40 to 7.41 Mg ha<sup>-1</sup>, and associated kriging standard errors ranged from 0.93 to 0.96 Mg ha<sup>-1</sup>.

A preliminary cotton yield response model was first developed using ordinary least squares (OLS) regression techniques. The physicochemical properties were the regressor or independent variables, and estimated yields were the response or dependent variable. A correlation analysis and scatter plots of yield vs. individual soil properties were used to develop the initial yield response model structure. This initial structure included linear effects for all 10 physicochemical properties. A backward variable selection procedure was used to screen out the clearly nonsignificant physicochemical parameters (parameters with *t*-score values below 1.8). This predictor screening procedure helped to alleviate the inherent multicollinearity between some of the predictor variables, specifically between SP and percentage clay and LF and Cl<sup>-</sup> data. Minimizing multicollinearity was also the reason for using  $\theta_v$  instead of volumetric water content because of the collinearity between  $\rho_b$  and volumetric water content. Based on this exploratory correlation analysis and preliminary multiple linear regression analysis, six primary soil properties were selected for the initial yield response model structure: EC<sub>e</sub>, LF, pH, percentage clay,  $\theta_p$ , and  $\rho_b$ .

The above-described data analysis and regression modeling were performed on the individual depth increment sample data (i.e., 0–0.3, 0.3–0.6, 0.6–0.9, 0.9–1.2, 1.2–1.5, and 1.5–1.8 m) and a variety of composite depth increments. No single soil layer or composite of layers rendered a better yield model than the 0- to 1.5-m depth increment; consequently, this was taken to represent the root zone of cotton at the study site. The preliminary regression modeling of cotton yield also showed that 1 of the 60 sample sites was consistently an outlier. The outlier was found to occur at a site intersecting the temporary east-west canal that was excavated to flood-irrigate the northern half of the field. This site was removed from all subsequent statistical analyses involving cotton yield. Figure 2 shows the east-west irrigation canal intersecting the eliminated sample site.

### Compensating for Spatial Autocorrelation

The development of functional relationships between crop productivity and yield-influencing factors with classical statistics such as OLS is only valid if the regression model residual errors can be shown to be spatially independent. However, when the residual errors are spatially correlated, OLS estimation techniques generally produce biased parameter estimates and test results (Cressie, 1993). Long (1998) demonstrated that autoregressive response modeling can be used to "diminish the adverse effects of autocorrelation on variance estimates and, thus, permit valid inferences concerning the dependence of *Y* (crop yield) on the *X* variables (factors influencing yield)." Spatial autocorrelation can also be adjusted with a maximum-likelihood approach (Littell et al., 1996).

An adjustment of the OLS cotton yield model for spatial autocorrelation was made using the maximum-likelihood ap-

proach implemented in the SAS (SAS Inst., 1999) PROC MIXED model-fitting procedure (Littell et al., 1996). Both the model parameter estimates and spatial error parameters were simultaneously estimated using this approach. In addition, the approximate statistical significance of the estimated spatial error parameters was determined using the likelihood test (Littell et al., 1996).

### Geographic Information System and Map Preparation

All spatial data were entered into a GIS using the commercial GIS software ArcView 3.1. Interpolated maps of the soil physicochemical properties were prepared by kriging the measurements. Previous studies comparing interpolation methods for mapping soil properties have found kriging better (Laslett et al., 1987; Warrick et al., 1988; Leenaers et al., 1990; Kravchenko and Bullock, 1999) while others have shown inverse distance weighting to be superior (Weber and Englund, 1992; Wollenhaupt et al., 1994; Gotway et al., 1996). Kriging was selected as the preferred method of interpolation because it was more accurate than inverse distance weighting based on the use of the mean squared error as the main criterion for comparison. Interpolated maps of the factors influencing cotton yield were prepared, and a map of the cotton yield was prepared by interpolation of the 7706 cotton yield sites.

## RESULTS AND DISCUSSION

Table 1 is a summary by depth of the soil physicochemical properties that potentially influence cotton yield variability at the study site. Soil salinity (EC<sub>e</sub>) increased with depth. The EC<sub>e</sub> reached as high as 37.5 dS m<sup>-1</sup> at the 1.5- to 1.8-m depth increment. There was a general spatial pattern of increasing salinity from south to north, with the highest salinity occurring in the northwest corner. Boron tended to follow the same general spatial patterns as salinity, increasing with depth through the soil profile, particularly in the northern third of the field. Levels as high as 45 mg L<sup>-1</sup> B were reached at the 1.5- to 1.8-m depth increment. With respect to texture, the soil was high in clay and fell primarily in the silty clay loam to clay loam textural range. In general, clay content tended to decrease with depth, and its spatial distribution showed a gradual increase in clay content from the southeastern corner to the northwestern corner of the study site at all depths. Gravimetric water content was higher at the deeper depths (i.e., 1.2–1.5 and 1.5–1.8 m) than the shallower depths but not substantially higher. Gravimetric water content followed a spatial pattern similar to that of percentage clay, gradually increasing from the southeast corner to the northwest corner for all depths. As expected, SP tended to closely correspond with the clay content. Soil reactivity or pH was quite stable at around 7.7 but tended to be slightly lower in the southwest corner and higher in the northeast corner. The highest pHs occurred at the 0.3- to 0.6-m depth increment. Nitrate N was highest in the 0- to 0.3-, 0.6- to 0.9-, and 0.9- to 1.2-m depth increments, with high pockets existing in the northern third and southern third of the study site. Bulk density was greatest at the 0.9- to 1.2-m depth and showed no discernible spatial trend.

Because the root zone was defined as 0 to 1.5 m, Table 2 presents basic statistical data for the averages

Table 1. Mean and range statistics of soil physicochemical properties for all depths (0–0.3, 0.3–0.6, 0.6–0.9, 0.9–1.2, 1.2–1.5, and 1.5–1.8 m).

Soil property†	No. of samples	Mean	Minimum	Maximum	Range	Standard deviation	Standard error	Coefficient of variation	Skewness	Kurtosis
<b>Depth 0–0.3 m</b>										
$\theta_p$ , kg kg <sup>-1</sup>	60	0.26	0.15	0.39	0.24	0.06	0.01	23.5	-0.13	-0.79
EC <sub>s</sub> , dS m <sup>-1</sup>	60	1.86	1.19	2.94	1.75	0.40	0.05	21.4	0.83‡	0.08
B, mg L <sup>-1</sup>	60	4.48	2.37	7.68	5.31	1.51	0.20	33.8	0.65‡	-0.69
pH	60	7.77	7.24	8.13	0.89	0.23	0.03	3.0	-0.27	-0.81
% clay	60	44.19	21.77	63.34	41.57	9.56	1.24	21.6	-0.65‡	-0.34
$\rho_b$ , Mg m <sup>-3</sup>	60	1.46	1.19	1.75	0.56	0.14	0.02	9.7	0.04	-0.93
NO <sub>3</sub> -N, mg L <sup>-1</sup>	60	43.21	8.10	122.99	114.89	19.13	2.47	44.3	1.35‡	3.94*
Cl <sup>-</sup> , mmol L <sup>-1</sup>	60	2.85	0.87	5.92	5.05	1.20	0.15	41.9	0.78‡	0.19
SP	60	60.90	39.77	74.93	35.16	8.80	1.14	14.5	-0.68‡	-0.48
<b>Depth 0.3–0.6 m</b>										
$\theta_p$ , kg kg <sup>-1</sup>	60	0.30	0.18	0.40	0.22	0.06	0.01	18.7	-0.42	-0.77
EC <sub>s</sub> , dS m <sup>-1</sup>	60	3.43	1.35	7.69	6.34	1.44	0.19	42.0	1.20‡	1.21
B, mg L <sup>-1</sup>	60	5.61	0	16.66	16.66	3.29	0.43	58.7	1.43‡	2.38‡
pH	60	7.84	6.85	8.30	1.45	0.25	0.03	3.2	-0.98‡	2.86‡
% clay	60	44.91	19.21	66.89	47.68	10.79	1.39	24.0	-0.71‡	-0.30
$\rho_b$ , Mg m <sup>-3</sup>	60	1.47	1.22	1.75	0.53	0.14	0.02	9.2	0.12	-0.92
NO <sub>3</sub> -N, mg L <sup>-1</sup>	60	12.05	0	63.01	63.01	15.86	2.05	131.6	1.32‡	1.01
Cl <sup>-</sup> , mmol L <sup>-1</sup>	60	7.46	0.79	23.06	22.27	4.12	0.53	55.2	1.18‡	2.40‡
SP	60	61.40	37.64	80.04	42.39	9.81	1.27	16.0	-0.72‡	-0.37
<b>Depth 0.6–0.9 m</b>										
$\theta_p$ , kg kg <sup>-1</sup>	60	0.28	0.15	0.37	0.22	0.06	0.01	20.7	-0.55	-0.71
EC <sub>s</sub> , dS m <sup>-1</sup>	60	6.61	1.58	17.65	16.07	5.00	0.65	75.6	0.99‡	-0.55
B, mg L <sup>-1</sup>	60	6.35	1.70	15.02	13.32	3.70	0.48	58.3	0.78‡	-0.47
pH	60	7.67	7.30	8.19	0.89	0.21	0.03	2.7	0.19	-0.50
% clay	60	39.39	13.31	60.93	47.62	12.23	1.58	31.0	-0.48	-0.82
$\rho_b$ , Mg m <sup>-3</sup>	60	1.57	1.36	1.80	0.44	0.09	0.01	6.0	0.06	0.21
NO <sub>3</sub> -N, mg L <sup>-1</sup>	60	29.28	0	134.31	134.31	27.95	3.61	95.5	1.39‡	2.42‡
Cl <sup>-</sup> , mmol L <sup>-1</sup>	60	9.25	2.49	18.56	16.07	3.50	0.45	37.8	0.35	-0.30
SP	60	55.08	31.91	75.43	43.52	11.15	1.44	20.2	-0.48	-0.78
<b>Depth 0.9–1.2 m</b>										
$\theta_p$ , kg kg <sup>-1</sup>	60	0.28	0.19	0.35	0.16	0.04	0.01	14.9	-0.20	-0.47
EC <sub>s</sub> , dS m <sup>-1</sup>	60	10.07	1.88	23.38	21.50	7.13	0.92	70.8	0.41	-1.39‡
B, mg L <sup>-1</sup>	60	8.51	2.00	20.98	18.98	5.61	0.72	65.9	0.62‡	-0.97
pH	60	7.63	7.17	8.18	1.01	0.19	0.03	2.5	-0.02	0.40
% clay	60	34.09	11.93	51.56	39.63	11.62	1.50	34.1	-0.28	-1.17
$\rho_b$ , Mg m <sup>-3</sup>	60	1.60	1.44	1.73	0.29	0.07	0.01	4.5	-0.12	-0.63
NO <sub>3</sub> -N, mg L <sup>-1</sup>	60	28.31	0	167.56	167.56	34.41	4.44	121.6	1.75‡	3.64‡
Cl <sup>-</sup> , mmol L <sup>-1</sup>	60	11.72	2.88	30.51	27.63	7.08	0.91	60.4	1.10‡	0.28
SP	60	50.19	30.28	64.28	34.00	9.73	1.26	19.4	-0.34	-1.04
<b>Depth 1.2–1.5 m</b>										
$\theta_p$ , kg kg <sup>-1</sup>	60	0.33	0.21	0.48	0.27	0.05	0.01	15.1	0.33	0.50
EC <sub>s</sub> , dS m <sup>-1</sup>	60	11.46	2.49	30.26	27.77	8.80	1.14	76.8	0.68‡	-1.02
B, mg L <sup>-1</sup>	60	9.69	2.26	24.59	22.33	6.44	0.83	66.4	0.70‡	-0.80
pH	60	7.71	7.28	8.24	0.96	0.22	0.03	2.9	0.05	-0.57
% clay	60	29.77	8.14	50.13	41.99	9.41	1.22	31.6	-0.25	-0.36
$\rho_b$ , Mg m <sup>-3</sup>	60	1.55	1.28	1.73	0.45	0.10	0.01	6.4	-0.47	0.49
NO <sub>3</sub> -N, mg L <sup>-1</sup>	60	11.93	0	97.91	97.91	23.11	2.98	193.7	2.12‡	3.79
Cl <sup>-</sup> , mmol L <sup>-1</sup>	60	17.34	3.73	67.31	63.58	14.77	1.91	85.2	1.63‡	2.38‡
SP	60	47.43	27.13	64.90	37.77	8.15	1.05	17.2	-0.32	-0.20
<b>Depth 1.5–1.8 m</b>										
$\theta_p$ , kg kg <sup>-1</sup>	43	0.37	0.24	0.47	0.23	0.05	0.01	14.3	-0.17	-0.38
EC <sub>s</sub> , dS m <sup>-1</sup>	43	15.31	2.13	35.68	33.55	10.68	1.63	69.8	0.26	-1.37
B, mg L <sup>-1</sup>	43	12.46	2.64	30.28	27.64	7.89	1.20	63.3	0.63	-0.63
pH	43	7.68	7.06	8.05	0.99	0.23	0.04	3.0	-0.38	-0.30
% clay	43	30.45	13.14	51.39	38.25	7.99	1.22	26.2	-0.23	0.23
$\rho_b$ , Mg m <sup>-3</sup>	43	1.53	1.28	1.73	0.45	0.09	0.01	5.9	-0.23	0.46
NO <sub>3</sub> -N, mg L <sup>-1</sup>	43	8.73	0	138.50	138.50	27.86	4.25	319.1	3.91‡	15.17‡
Cl <sup>-</sup> , mmol L <sup>-1</sup>	43	28.92	3.57	145.60	142.03	31.59	4.82	109.2	1.64‡	2.96‡
SP	43	48.33	31.29	67.98	36.69	7.09	1.08	14.7	-0.33	0.90

†  $\theta_p$ , gravimetric water content; EC<sub>s</sub>, electrical conductivity of the saturation extract;  $\rho_b$ , bulk density; SP, saturation percentage.

‡ Significant. Skewness is significant if skewness divided by standard error of skewness > 2. Kurtosis is significant if kurtosis divided by standard error of kurtosis > 2.

of the top 1.5 m of soil at each of the 60 sites. Nitrate N consistently had the highest coefficient of variation, which indicates high spatial variability across the field (see Tables 1 and 2). Electrical conductivity of the saturation extract, B, and Cl<sup>-</sup> showed considerable variability as reflected by coefficients of variation consistently near or above 40, except in the top 0 to 0.3 m. The pH and  $\rho_b$  values consistently showed the lowest coefficients of variation. Leaching through the root zone (0–1.5 m), as quantified by the LF, was the highest in a broad band

that extended west to east through the middle of the field. Another pocket of high leaching occurred in the southwest corner. Overall, the LF for the entire field was 0.28 with considerable variability across the field (CV = 64.6).

### Preliminary Correlation Analysis

The calculation of simple correlation coefficients of spatially varying soil properties to field-scale yield is a

**Table 2. Soil physicochemical property mean and range statistics of the averages over depths 0 to 1.5 m at each of the 60 sites.**

Soil property†	No. of sites	Mean	Minimum	Maximum	Range	Standard deviation	Standard error	Coefficient of variation	Skewness	Kurtosis
Depth 0–1.5 m										
$\theta_p$ , kg kg <sup>-1</sup>	60	0.29	0.18	0.37	0.19	0.05	0.01	16.0	-0.42	-0.60
EC <sub>e</sub> , dS m <sup>-1</sup>	60	6.68	2.13	15.06	12.93	4.36	0.56	65.2	0.69‡	-0.99
B, mg L <sup>-1</sup>	60	6.93	2.48	16.29	13.81	3.96	0.51	57.1	0.73‡	-0.68
pH	60	7.73	7.21	8.12	0.91	0.18	0.02	2.4	-0.38	-0.11
% clay	60	38.47	18.10	55.83	37.73	9.99	1.29	26.0	-0.55	-0.90
$\rho_b$ , Mg m <sup>-3</sup>	60	1.53	1.40	1.67	0.27	0.06	0.01	4.2	-0.16	-0.64
NO <sub>3</sub> -N, mg L <sup>-1</sup>	60	24.96	4.52	76.74	72.21	17.58	2.27	70.4	1.26‡	0.98
Cl <sup>-</sup> , mmol L <sup>-1</sup>	60	9.73	3.49	25.02	21.53	5.06	0.65	52.0	1.31‡	1.22‡
SP	60	55.00	37.09	68.18	31.09	8.78	1.13	16.0	-0.61	-0.89
LF§	60	0.28	0.04	0.77	0.73	0.18	0.02	64.6	0.67‡	-0.24

†  $\theta_p$ , gravimetric water content; EC<sub>e</sub>, electrical conductivity of the saturation extract;  $\rho_b$ , bulk density; SP, saturation percentage; LF, leaf fraction.

‡ Significant. Skewness is significant if skewness divided by standard error of skewness > 2. Kurtosis is significant if kurtosis divided by standard error of kurtosis > 2.

§ Leaf fraction was determined by dividing the Cl<sup>-</sup> concentration of the irrigation water by the Cl<sup>-</sup> concentration of the saturation extract at the 1.2- to 1.5-m depth increment at each of the sites.

first-step approach in explaining yield variation but is usually not sufficient. This is because correlations provide little direct evidence for the cause(s) of yield variation and because correlation analysis is an assessment of the linear relationship between variables, which does not account for nonlinear relationships or multiple, interacting, yield-affecting factors (Kitchen et al., 1999). Nevertheless, simple correlations do provide the first level of information needed to determine what factors are influencing yield.

The correlation coefficient ( $r$ ) for EC<sub>e</sub> and yield was  $r = 0.51$  ( $P < 0.01$ ). Because EC<sub>e</sub> is a measure of several soil properties, the moderate positive correlation of EC<sub>e</sub> and yield suggests that either the interaction of these properties was significant in influencing cotton yield or that one or two properties influenced yield and the others were collinear. Even though the correlation between EC<sub>e</sub> and yield was significant, there were obviously other factors influencing yield beyond those measured by EC<sub>e</sub>. Nevertheless, at this particular study site, EC<sub>e</sub> was a useful indicator of cotton yield.

The results from preliminary correlation analysis between EC<sub>e</sub> and soil properties are shown in Table 3. Electrical conductivity of the saturation extract, B,  $\theta_p$ , percentage clay, and SP are highly correlated with the EC<sub>e</sub>, with correlation coefficients of 0.87, 0.88, 0.79, 0.76, and 0.77, respectively (Table 3). However, B is not a property measured by EC<sub>e</sub>. The high correlation of B to EC<sub>e</sub> is an artifact due to its close correspondence to salinity (i.e., EC<sub>e</sub>) as a result of the process of leaching. The correlation coefficient between B and EC<sub>e</sub> was 0.96. The high correlation of EC<sub>e</sub> to both percentage clay and SP is expected because it reflects the influence of texture on the EC<sub>e</sub> reading and because percentage clay and SP are highly correlated ( $r = 0.99$ ). In this particular field, EC<sub>e</sub> is highly correlated with salinity,  $\theta_p$ , and texture.

Table 3 also shows the correlation between cotton yield and selected soil properties. The highest correlation between yield and a single soil property was for salinity (EC<sub>e</sub>). A scatter plot of EC<sub>e</sub> and yield exhibited a quadratic relationship with the predicted yield levels increasing and then falling off (Fig. 4a). The yield data displayed a negative, curvilinear relationship with the LF (Fig. 4b). The yield tended to display minimal response to LF values <0.4 and then fall off rapidly for LF values >0.4. Clay percentage, pH,  $\theta_p$ , and  $\rho_b$  appear to be linearly related with the yield data to various de-

gress (Fig. 4c, 4e, and 4f). Even though there is no correlation between yield and pH ( $r = -0.01$ ; see Fig. 4d), pH became statistically significant in the presence of the other variables in the final yield response model. Although the absolute soil water content is clearly time dependent, the relative spatial patterns of water content variation (i.e., hydrologic signatures) remain fairly constant over the growing season (Engman, 1999). This suggests that the  $\theta_p$  data can serve as a surrogate variable indicating the relative level of plant-available water. The high correlation between percentage clay and  $\theta_p$  ( $r = 0.90$ ) and between percentage clay and calculated water content at field capacity ( $r = 0.79$  where field capacity = SP/2; Rhoades et al., 1999a) suggests that hydrologic signatures are reasonably stable at this study site.

Boron was positively correlated with yield and was linear. The positive, linear relationship between B and yield suggests no yield decrement effect for the range of observed root-zone B concentrations (2.45–16.29 mg L<sup>-1</sup>). Even though the average root-zone B concentration exceeded the cited threshold limit of 10 mg L<sup>-1</sup> at 12 locations (Maas, 1984), there was no noticeable yield decrement. Ostensibly, the B concentration in the top 0.9 m of soil, which in all cases was <10 mg L<sup>-1</sup>, was

**Table 3. Correlation coefficients calculated for selected soil physicochemical properties and apparent soil electrical conductivity (EC<sub>e</sub>) and selected soil physicochemical properties and yield.**

Physicochemical property†	Fixed-array EC <sub>e</sub> ‡	Yield§
$\theta_p$ ¶	0.79**	0.42**
EC <sub>e</sub> ¶	0.87**	0.53**
B¶	0.88**	0.50**
pH¶	0.33*	-0.01
% clay¶	0.76**	0.36*
$\rho_b$ ¶	-0.38**	-0.29*
NO <sub>3</sub> -N¶	0.22	-0.03
Cl <sup>-</sup> ¶	0.61**	0.25*
LF#	-0.50**	-0.49**
SP¶	0.77**	0.38*

\* Significant (test for  $|r| = 0$ ) at the  $P \leq 0.05$  level.

\*\* Significant (test for  $|r| = 0$ ) at the  $P \leq 0.01$  level.

†  $\theta_p$ , gravimetric water content; EC<sub>e</sub>, electrical conductivity of the saturation extract;  $\rho_b$ , bulk density; LF, leaching-fraction; SP, saturation percentage.

‡ Pearson correlation coefficients based on 60 observations.

§ Pearson correlation coefficients based on 59 observations.

¶ Averaged over 0 to 0.15 m.

# Leaching fraction was determined by dividing the Cl<sup>-</sup> concentration of the irrigation water by the Cl<sup>-</sup> concentration of the saturation extract at the 1.2- to 1.5-m depth increment at each site.

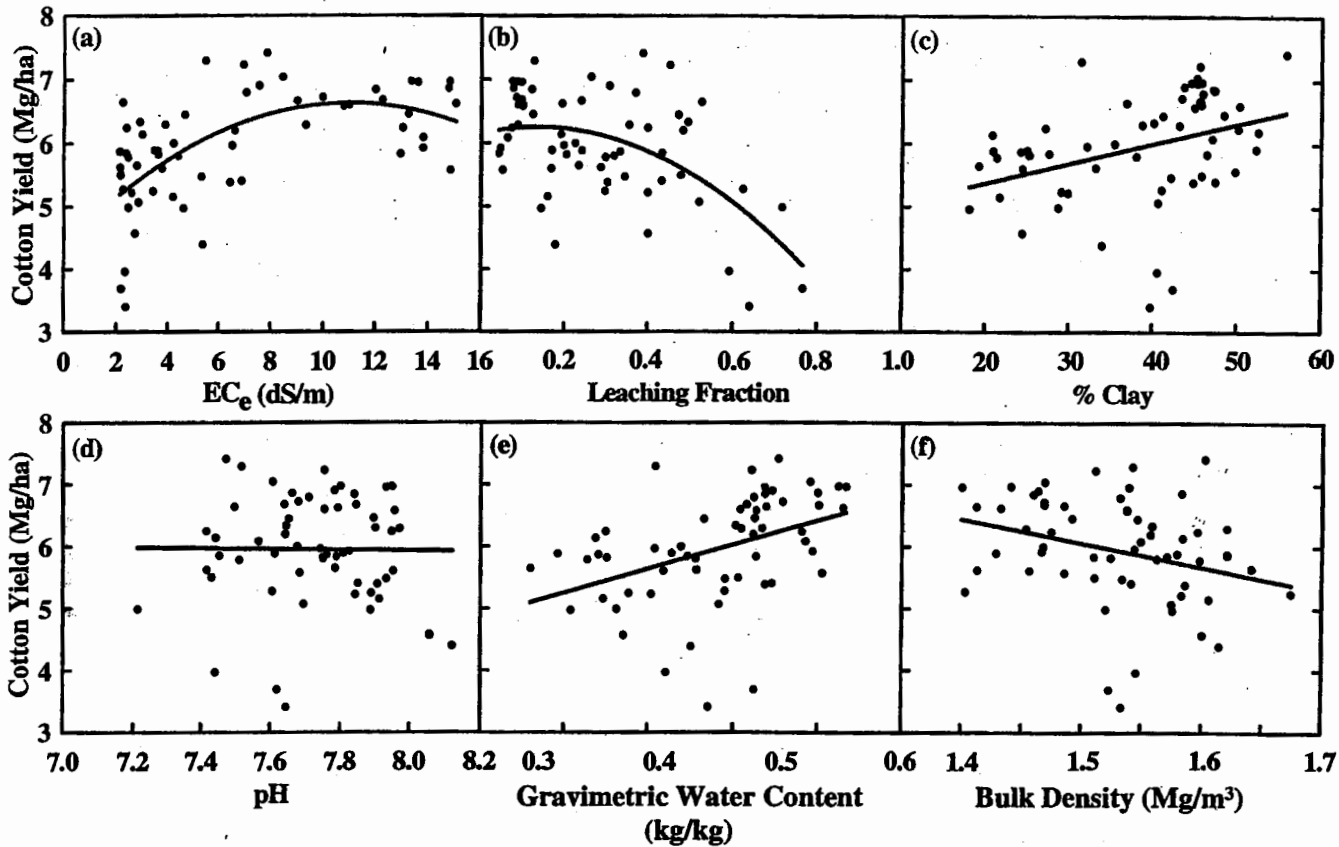


Fig. 4. Scatter plots of selected soil properties and cotton yield: (a) electrical conductivity of the saturation extract ( $EC_e$ ,  $dS m^{-1}$ ), (b) leaching fraction, (c) percentage clay, (d) pH, (e) gravimetric water content ( $kg kg^{-1}$ ), and (f) bulk density ( $Mg m^{-3}$ ).

sufficiently low to prevent any B toxicity from occurring (Maas, 1984).

### Crop Yield Response Model

Based on initial exploratory correlation and multiple linear regression analysis, the following regression model structure was proposed for describing the soil property effects on cotton yield:

$$Y = \beta_0 + \beta_1(EC_e) + \beta_2(EC_e)^2 + \beta_3(LF)^2 + \beta_4(pH) + \beta_5(\text{percentage clay}) + \beta_6(\theta_g) + \beta_7(\rho_b) + \epsilon \quad [2]$$

where, based on Fig. 4, the relationships between cotton yield ( $Y$ ) and pH, percentage clay,  $\theta_g$ , and  $\rho_b$  are assumed to be linear; the relationship between yield and  $EC_e$  is assumed to be quadratic; the relationship between yield and LF is assumed to be curvilinear;  $\beta_0, \beta_1, \beta_2, \dots, \beta_7$  are the regression model parameters; and  $\epsilon$  represents the random error component, initially assumed to be normally distributed and spatially independent.

Table 4 shows the OLS regression modeling summary results for Eq. [2]. The  $R^2$  value of 0.61 suggests that Eq. [2] successfully described slightly more than 60%

Table 4. Ordinary least-squares regression statistics for Eq. [2].†

Significant regressor variables‡	Regressor coefficients	Standard error	df	t	P >  t
Constant	20.90	4.19	1	4.99	<0.0001
$EC_e$ , $dS m^{-1}$	0.38	0.14	1	2.68	0.010
$EC_e^2$ , $dS m^{-1}$	-0.02	0.01	1	-2.97	0.005
$LF^2$	-3.51	1.07	1	-3.29	0.002
pH	-2.22	0.50	1	-4.44	<0.0001
% clay	-0.02	0.02	1	-0.89	0.379
$\theta_g$ , $kg kg^{-1}$	9.27	4.77	1	1.94	0.058
$\rho_b$ , $Mg m^{-3}$	-0.32	1.50	1	-0.22	0.829
Analysis of variance					
Source	Sum of squares	df	Mean square	F ratio	P > F
Model	26.67	7	3.81	11.25	<0.0001
Error	17.27	51	0.34		
Corrected total	43.94	58			

† Dependent variable = yield ( $Mg ha^{-1}$ ), number of data points = 59, root mean square error = 0.58,  $R^2 = 0.61$ , and adjusted  $R^2 = 0.55$ .

‡  $EC_e$ , electrical conductivity of the saturation extract; LF, leaf fraction;  $\theta_g$ , gravimetric water content;  $\rho_b$ , bulk density. All variables are for the 0- to 1.5-m depth increment.

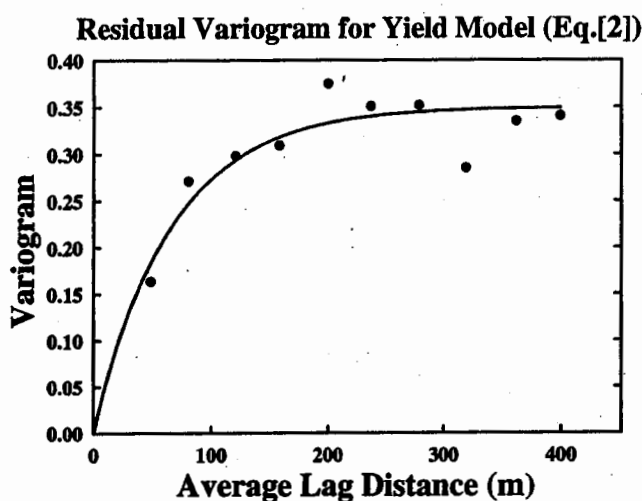


Fig. 5. Residual variogram for ordinary least-squares yield regression model (Eq. [2]). The points are the experimental variogram for the 59 points while the solid line represents the fitted variogram.

of the estimated spatial yield variation. The nonsignificant  $t$  tests associated with the percentage clay and  $\rho_b$  parameter estimates suggest that these soil properties do not contribute to the yield predictions in a statistically meaningful manner. However, all of the other parameters appear to be significant near or below the 0.05 level.

An analysis of the regression model residuals revealed no outliers. The normal distribution assumption appeared valid, and the residuals passed the Shapiro-Wilk Normality Test (Shapiro and Wilk, 1965). However, as shown in Fig. 5, the residual variogram plot indicates that the errors were spatially correlated. This implies that optimal, unbiased estimates of the regression model parameters cannot be obtained using OLS fitting techniques. Instead, an adjustment for the spatially correlated error structure must be employed during the estimation of this model.

Using a restricted maximum likelihood approach, both the model parameter estimates and spatial error parameters were simultaneously estimated in an objective manner. In addition, the approximate statistical significance of the stimulated spatial error parameters was de-

Table 5. Maximum likelihood estimation results for Eq. [2].†

Effect‡	Solution for fixed effects				
	Estimate	Standard error	df	$t$ test	$P >  t $
Constant	18.21	5.14	0	3.55	
$EC_e$ , dS m <sup>-1</sup>	0.25	0.13	51	1.88	0.066
$EC_e^2$ , dS m <sup>-1</sup>	-0.02	0.01	51	-2.43	0.019
LF <sup>2</sup>	-4.26	0.95	51	-4.47	<0.0001
pH	-2.04	0.58	51	-3.52	0.001
% clay	-0.01	0.02	51	-0.61	0.544
$\theta_p$ , kg kg <sup>-1</sup>	8.85	4.07	51	2.18	0.034
$\rho_b$ , Mg m <sup>-3</sup>	0.78	1.33	51	0.59	0.560

† Model Information: dependent variable = yield (Mg/ha), covariance structure = spatial exponential (no nugget), and estimation method = restricted maximum likelihood; Dimensions: covariance parameters = 2, regression model parameters = 8, and total observations = 59; Fitting Information: -2 res log likelihood = 102.5 (note: -2 res log likelihood value for an identical model with iid error structure = 111.3); Covariance Parameter Estimates: spatial exponential covariance structure (range) = 68.17 and residual (MSE) = 0.41.

‡  $EC_e$ , electrical conductivity of the saturation extract; LF, leaf fraction;  $\theta_p$ , gravimetric water content;  $\rho_b$ , bulk density.

termined using a likelihood ratio test (Littell et al., 1996). Table 5 shows the recalculated parameter estimates using an assumed isotropic exponential spatial covariance structure with no nugget and one adjustable range parameter. The adjusted  $t$ -test results still indicate that the percentage clay and  $\rho_b$  can be removed from the regression model. The likelihood ratio test statistic for the spatial covariance structure yielded a Chi-square value of 8.8 (see Table 5; 111.3 - 102.5 = 8.8) with 1 degree of freedom ( $p = 0.003$ ), indicating that the errors are spatially correlated.

The removal of percentage clay and  $\rho_b$  from Eq. [2] resulted in the most robust and parsimonious yield response model for cotton. Table 6 shows the final maximum likelihood parameter estimates after removing percentage clay and  $\rho_b$ , which results in the following yield response model:

$$Y = 19.277 + 0.218(EC_e) - 0.015(EC_e)^2 - 4.420(LF)^2 - 1.991(pH) + 6.927(\theta_g) + \epsilon \quad [3]$$

The LF<sup>2</sup> and pH parameters are highly significant, and the  $EC_e$  (linear and quadratic) and  $\theta_g$  parameter estimates are significant at or near the 0.05 level. The LF<sup>2</sup> and pH parameters are both negative, implying that the yield decreased as either the LF or soil pH increased. The  $\theta_g$  term is positive, implying that the yield increased as the plant-available water content increased. The positive linear and negative quadratic  $EC_e$  terms imply that the yield increased under low salinity but decreased under higher salinity levels. The point of maximum yield with respect to salinity was calculated by setting the first partial derivative of the fitted regression to zero with respect to  $EC_e$ , which resulted in a value of 7.17 dS m<sup>-1</sup>. This is very similar to the salinity threshold for cotton of 7.7 dS m<sup>-1</sup> reported by Maas and Hoffman (1977).

Table 6 also shows the estimated sill (mean square error) and range parameters for the assumed exponential spatial covariance structure. The maximum likelihood estimate of the mean square error was 0.39, indicating that the root mean square error is about 0.63 Mg ha<sup>-1</sup> for this model. The range parameter estimate was about 66.2 m, indicating that the range of residual spatial correlation was less than the corresponding raw yield

Table 6. Maximum likelihood estimation results for Eq. [3].†

Effect‡	Solution for fixed effects				
	Estimate	Standard error	df	$t$ test	$P >  t $
Constant	19.28	4.57	0	4.22	
$EC_e$ , dS m <sup>-1</sup>	0.22	0.11	53	1.91	0.061
$EC_e^2$ , dS m <sup>-1</sup>	-0.02	0.01	53	-2.51	0.015
LF <sup>2</sup>	-4.42	0.87	53	-5.10	<0.0001
pH	-1.99	0.57	53	-3.52	0.001
$\theta_p$ , kg kg <sup>-1</sup>	6.93	3.07	53	2.26	0.028

† Model Information: dependent variable = yield (Mg/ha), covariance structure = spatial exponential (no nugget), and estimation method = restricted maximum likelihood; Dimensions: covariance parameters = 2, regression model parameters = 8, and total observations = 59; Fitting Information: -2 res log likelihood = 99.5; Covariance Parameter Estimates: spatial exponential covariance structure (range) = 66.22 and residual (MSE) = 0.39.

‡  $EC_e$ , electrical conductivity of the saturation extract; LF, leaf fraction;  $\theta_p$ , gravimetric water content.

spatial correlation range of 109.3 m but still statistically significant.

Figure 6 displays the final observed vs. predicted cotton yield estimates while Fig. 7 compares maps of measured cotton yields and predicted yields based on Eq. [3]. Figure 6 suggests that the estimated regression relationship has been reasonably successful at reproducing the predicted yield estimates. Figure 7 shows a reasonably close spatial association between interpolated measured and predicted maps.

### Interpretation of Soil Properties' Influence on Cotton Yield

The quadratic relationship between  $EC_e$  and yield (Fig. 4a) is not in line with the piece-wise linear response function between salinity and yield commonly presented in the literature (Maas and Hoffman, 1977). The traditional two-piece linear response function consists of a tolerance plateau with a slope of zero and a salinity-dependent line whose slope indicates the yield reduction per unit increase in salinity (Maas and Hoffman, 1977). The point of intersection of the two lines designates the salinity threshold. An explanation for the disparity may be overleaching. Several of the sample sites where low yield (i.e.,  $<5.5 \text{ Mg ha}^{-1}$ ) corresponded with low  $EC_e$  (i.e.,  $<3 \text{ dS m}^{-1}$ ) also had low  $\text{NO}_3\text{-N}$  (i.e.,  $<5 \text{ mg L}^{-1}$ ) levels accompanied with high leaching (i.e.,  $LF > 0.5$ ). This suggests that overleaching may have been responsible for the removal of  $\text{NO}_3\text{-N}$ , particularly in the southwest corner of the study area (Fig. 8a and 8b), which led to low yield. The low yield associated with low salinity is an artifact rather than a cause-and-effect relationship.

The degree of influence that each soil property had on the cotton yield as indicated by Eq. [3] is shown in Table 7. This influence was determined by calculating

how much the predicted yield decreased when the value for each soil property was individually shifted up (or down) by 1 standard deviation from its mean level. A baseline value of 7.17 was used for salinity, rather than the mean  $EC_e$  level of 6.72, because 7.17 represents the point of maximum yield with respect to the quadratic salinity response pattern. The calculated percentage yield reduction data shown in Table 7 indicates that LF is the most significant factor influencing yield.

The observed spatial patterns of LF in the northern and southern halves of the field (see Fig. 8b) are largely the consequence of flood irrigation distributions and the temporary unlined irrigation canal. The field is a leveled field with a gradual downhill slope ( $0.0009 \text{ m m}^{-1}$ ) from the southwest to the northeast. A temporary east-west irrigation canal is located at the southern end of the field with the irrigation water source entering at the southwest corner and a temporary irrigation canal running north to south along the west side from the southwest corner to midfield and then running west to east at midfield (see Fig. 2). The temporary canals were excavated after planting and filled before harvest. From these temporary canals, the field was flood-irrigated in two sections: the northern half and the southern half. Flood irrigation occurs over north-south furrows.

With respect to the northern half of the field, high leaching in the vicinity of the temporary irrigation canal (i.e., the east-west midfield portion of the canal) and progressively lower leaching from south to north are the consequence of uncontrolled leaching from the unlined canal and flood irrigation down the north-south furrows from the midfield canal, respectively. The uneven water distribution from south to north is a consequence of the time for water to travel down the furrows and reach the end of the field; consequently, greater applied water, infiltration, and leaching occurred near midfield closest to the irrigation source (i.e., the east-west canal) with diminished applied water from south to north.

The observed spatial patterns of LF in the southern half of the field shows greater leaching on the west side than on the east side with no noticeable north-south trends. The east-west spatial patterns of LF are similar to the general east-west patterns of percentage clay with decreasing clay content from west to east. The fact that greater leaching occurred where fine-textured soil is present is unexpected and more likely reflects nonuniformity of water application from west to east due to flood irrigation. The nonuniform water application is the consequence of higher volumes of water being applied on the west side of the field closest to the source of irrigation water and nearest to the unlined north-south canal.

A potential cause-and-effect explanation for the inverse relationship of yield to LF may also relate to overleaching. Intuitively, areas receiving larger amounts of water would most likely produce higher yields unless the areas of lowest leaching were receiving sufficient water to meet water needs and areas of high leaching were being overleached. Overleaching would be a consequence of applying more water than needed for the particular soil texture. Coarse-textured soils require less wa-

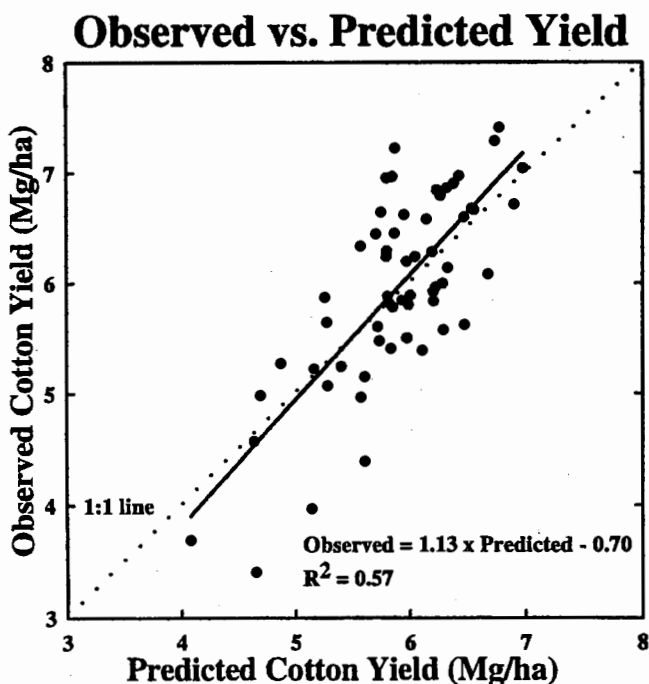


Fig. 6. Observed vs. predicted cotton yield estimates using Eq. [3]. Dotted line is a 1:1 relationship.

# Measured vs. Predicted Cotton Yield

(interpolated data)

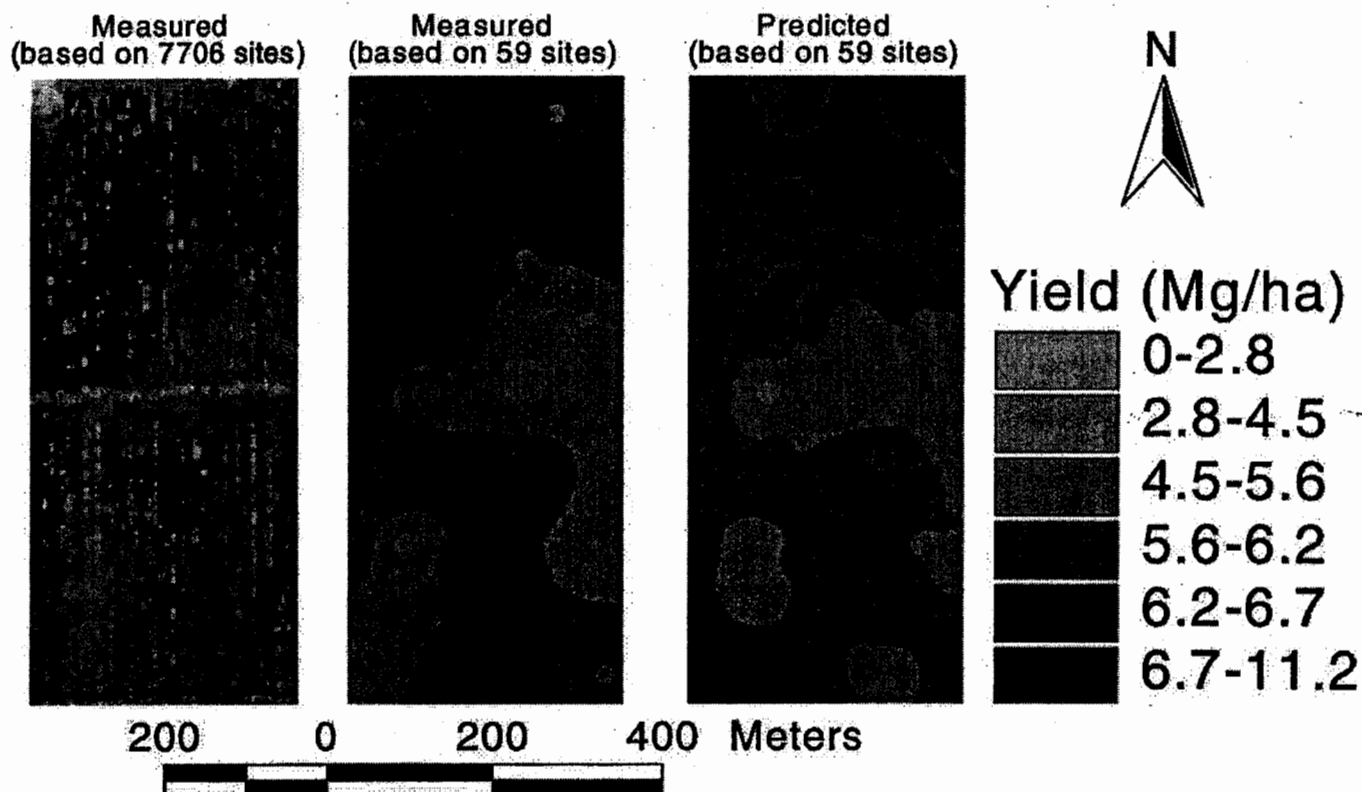


Fig. 7. Comparison of measured cotton yield based on 7706 yield measurements, kriged data at 59 sites for measured cotton yield, and kriged data at 59 sites for predicted cotton yields based on Eq. [3].

ter to reach field capacity than fine-textured soils. Over-leaching would remove important mobile nutrients. Evidence of overleaching is reflected by the field's negative correlation between LF and  $\text{NO}_3\text{-N}$  ( $r = -0.52$ ).

An interpretation of how and why the remaining two soil properties, pH and  $\theta_g$ , influence yield provides further insight into the crop response dynamics. Soil pH has a negative parameter estimate, indicating an inverse relationship with yield, while  $\theta_g$  has a positive relationship (Table 6). The relationship between yield and  $\theta_g$  reflects the positive response of the plant to higher available water. Over the range of encountered root-zone pHs (7.21–8.12), an increase in the pH slightly decreased the yield. Potential reasons for the slight decrease in yield with increasing pH are (i) the solubility of cationic trace elements decreases with increasing pH, so plant deficiencies of Cu, Fe, Mn, and Zn commonly exist at higher pH in saline soils (Page et al., 1990) and (ii) high pHs can cause soil infiltration problems (Suarez et al., 1984), thereby reducing water availability.

Because of the close positive correlation between B and salinity ( $r = 0.96$ ), it is difficult to separate out the yield reduction effect of salinity and B. It could be argued that B rather than salinity was influencing cotton yield or that both in combination were influencing yield. The root-zone threshold levels of salinity and B are

$7.7 \text{ dS m}^{-1}$  (Maas and Hoffman, 1977) and  $10 \text{ mg L}^{-1}$  (Maas, 1984), respectively, for cotton. The average root-zone salinity in 20 locations was  $>7.7 \text{ dS m}^{-1}$ . The average root-zone B concentration exceeded  $10 \text{ mg L}^{-1}$  at 14 locations. However, exploratory correlation analysis showed no influence of B on cotton yield. Furthermore, the fact that B was eliminated by backward elimination procedures from exploratory model variable selection suggests that there is no statistical evidence for the reduction of cotton yield by B.

## SUMMARY AND CONCLUSION

Crop yield monitoring with continuous-flow sensors and GPS indicate areas within fields that differ in crop productivity. Yield maps provide the basis for implementing site-specific crop management by indicating where varying cropping inputs are needed based on spatial patterns of crop productivity (Long, 1998). However, the cropping inputs necessary to optimize productivity and minimize environmental impacts can be derived only if it is known what factors gave rise to the observed spatial crop patterns (Long, 1998). Edaphic properties comprise one set of factors influencing crop patterns. The  $\text{EC}_a$  measurement is influenced by several soil properties that also influence cotton yield on arid-zone soils

## Factors Influencing Cotton Yield

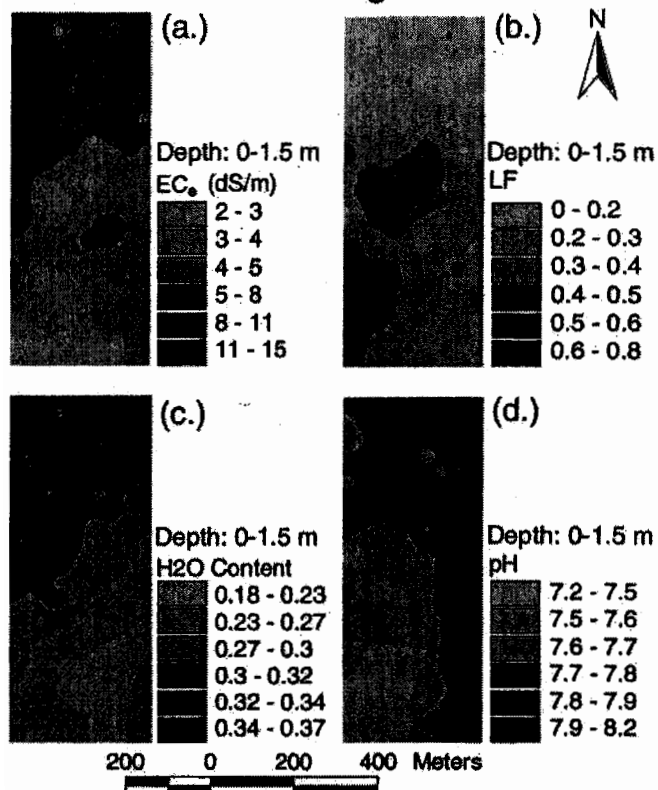


Fig. 8. Maps of the four most significant factors (0–1.5 m) influencing cotton yield: (a) electrical conductivity of the saturation extract ( $EC_e$ ,  $dS\ m^{-1}$ ), (b) leaching fraction (LF), (c) gravimetric water content ( $kg\ kg^{-1}$ ), and (d) pH.

in the San Joaquin Valley: salinity ( $EC_e$ ), volumetric water content,  $\rho_b$ , and clay content. Hypothetically, when crop yield correlates with  $EC_e$ , spatial distributions of  $EC_e$  provide a potential means of determining soil properties that influence yield. This hypothesis was evaluated. A yield map would provide this same capability, but because yield monitoring has not been developed for all crops,  $EC_e$  maps provide a viable alternative when yield-monitoring data are not available.

From a practical perspective, the key to determining the soil properties that influence crop yield is a sample design that minimizes the number of samples but spatially characterizes the soil properties influencing yield. Rapid and easily obtained spatial measurements of  $EC_e$  provide a means of determining the soil properties that influence cotton yield by serving as covariate spatial information for directing soil sample design. This approach minimizes an otherwise intensive grid sampling

of multiple soil parameters with a sample design optimized for the characterization of crop yield and soil heterogeneity. The presented approach provides a means of identifying within a field the predominant soil properties that influence cotton yield through the correlation of various soil properties and cotton yield at points that characterize the field's full range of yield and properties influencing that yield. However, this is just one piece to the puzzle because yield is influenced by a complex interaction of meteorological (humidity, temperature, etc.), biological (e.g., pests), anthropogenic (management related), and edaphic (soil related) factors. Nevertheless, knowing the site-specific edaphic influences on crop yield provides a layer of information useful in its site-specific management. By knowing the soil properties that influence a crop's yield, recommendations can be made to improve productivity. Based on Eq. [3], cotton yield at the Broadview Water District study site can hypothetically be improved by

1. reducing the LF in highly leached locations (i.e., areas where  $LF > 0.5$ ),
2. reducing salinity by increased leaching in areas where the average root-zone (0–1.5 m) salinity was  $> 7.17\ dS\ m^{-1}$ ,
3. increasing the plant-available water,
4. and reducing the pH.

All four recommendations can be accomplished by improved water application timing and distribution and precision application of soil amendments. By improving the water application distribution and timing, (i) areas with high LF (i.e.,  $LF > 0.5$ ) can receive less water; (ii) areas with average root-zone salinity  $> 7.17\ dS\ m^{-1}$  can be leached more heavily; and (iii) coarse-textured soils with low plant-available water (i.e.,  $\theta_s < 0.3\ g\ g^{-1}$ ) can be irrigated more frequently. Areas of high pH (i.e.,  $pH > 8$ ) can be lowered with the addition of a soil amendment (e.g., organic matter, acid, sulfur). Clearly, the delineation of site-specific management units based on this information can be accomplished with the overlay capability in a GIS.

The presented approach provides spatial information for use in soil and crop management. The aforementioned recommendations reflect the importance of irrigation management and efficiency to cotton yield on arid-zone soils of the San Joaquin Valley. As indicated, spatial distribution and frequency of applied irrigation water are important factors in cotton yield by controlling leaching of  $NO_3-N$ , salt accumulation in the root zone, and available water to the plant. The results suggest that irrigation water needs to be applied at a higher frequency

Table 7. Degree of predicted yield sensitivity to 1 standard deviation (SD) change in each soil property of Eq. [3].

Parameter sensitivity†	Calculated yield	Percentage reduction	$EC_e$	$LF$	$pH$	$\theta_s$
			$dS\ m^{-1}$			$kg\ kg^{-1}$
Baseline	6.33		7.17	0.28	7.73	0.29
$EC_e + 1\ SD$	6.04	4.6	11.56	0.28	7.73	0.29
$LF + 1\ SD$	5.72	9.6	7.17	0.47	7.73	0.29
$pH + 1\ SD$	5.96	5.8	7.17	0.28	7.91	0.29
$\theta_s + 1\ SD$	6.01	5.1	7.17	0.28	7.73	0.24

†  $EC_e$ , electrical conductivity of the saturation extract; LF, leaf fraction;  $\theta_s$ , gravimetric water content.

in areas of a field that have lower plant-available water (i.e., generally more sandy-textured soils), whereas soils high in clay with higher plant-available water need less frequently applied water. Furthermore, an efficient spatial distribution of water application is needed that optimizes leaching. Optimal leaching provides sufficient water at a location to optimize crop yield while minimizing environmental impacts and unnecessary depletion of water resources. This is achieved by (i) providing sufficient water to meet evapotranspiration and leaching needs; (ii) minimizing overleaching of nutrients, which reduces yield and detrimentally impacts ground water and drainage water; and (iii) adequately leaching areas that are above the salinity threshold for the crop. All of these require accurate spatial information on crop water use.

Adjustments to the application of irrigation water within a field can be based on the analysis and interpretation of spatial soil data as presented in this study. However, the ability to control the application of irrigation water to delineated management units within a field is limited. Commercially available irrigation systems capable of within-field application control at a cost-effective price are currently unavailable. Nevertheless, conventional sprinkler and flood irrigation systems can still benefit from this spatial soil information provided simple modifications are made to the irrigation system. Stationary sprinkler systems can be outfitted with valves at each sprinkler head to control frequency and distribution of application. Maps of plant-available water and salinity distribution can then be used to adjust by hand the volume and frequency of irrigation water application. In areas where flood irrigation occurs, more uniform application of irrigation water can be achieved through shorter runs that minimize over- and underleaching. The locations of shorter or longer runs and the volume of water applied within each furrow can be established from the maps of soil properties influencing cotton yield. The presented GIS-based approach provides the maps that make this level of irrigation management and efficiency possible from a strictly informational standpoint.

As a cautionary note, there are definite limitations to the site-specific information that can be derived from Eq. [3]. First, it is apparent from the moderate  $R^2$  value for Fig. 6, which compares observed and predicted yields as calculated from Eq. [3], that there are factors (biological, meteorologic, and anthropogenic) influencing yield other than those identified in the equation. The full range of influence of these factors on the identified edaphic factors is unknown. For instance, increases in humidity or  $\text{CO}_2$  could drastically alter the influence of the edaphic factors and their interrelationship as quantified in Eq. [3]. Second, the robustness of Eq. [3] is limited because of the noise in the yield data, which is a function of the yield monitor and combine dynamics. Furthermore, because Eq. [3] was developed from one observational field study without any experimental control over the state variables, it is not sufficiently robust to use in an explicit calculation of  $\text{EC}_a$ , LF,  $\theta_v$ , and pH values that will optimize cotton yield at point locations within the field. Rather, the yield model serves as an implicit indicator of those factors that can be adjusted,

over the range of their measured occurrence within the field, to improve yield.

It is well known that the exclusive use of  $\text{EC}_a$  maps to explain yield variability is ineffective. Even though a crop yield map is the best indicator of all factors influencing yield because it encompasses edaphic, anthropogenic, biological, and meteorological factors, the interactions of these factors are too complex to derive site-specific management recommendations. Crop yield maps by themselves are of limited utility because of the difficulty in isolating the influence of each factor. However, a map of  $\text{EC}_a$  can be used in soil sample design to help isolate soil-related factors and specific anthropogenic factors (i.e., leaching efficiency), which influence yield heterogeneity, thereby providing an initial level of understanding for making site-specific management recommendations. Furthermore, crop yield maps are not always obtainable because yield-monitoring equipment has not been developed for all crops, but a map of  $\text{EC}_a$  can always be obtained. In general, exclusive use of a yield or  $\text{EC}_a$  map by itself is not sufficient to understand the reason(s) for yield variability in a field. Each is a piece to the puzzle of understanding the cause-and-effect factors influencing the spatial variation of a crop's yield.

#### ACKNOWLEDGMENTS

The authors acknowledge the outstanding work of Jack Jobs and JoAn Fargerlund, who performed the field soil sample collection and laboratory analyses. Their scientific experience, knowledge, and diligence in the field and laboratory were crucial to the success of this project.

#### REFERENCES

- Atherton, B.C., M.T. Morgan, S.A. Shearere, T.S. Stombawgh, and A.D. Ward. 1999. Site-specific farming: A perspective on information needs, benefits, and limitations. *J. Soil Water Conserv.* 54(2): 455-461.
- Black, C.A. 1968. Soil-plant relationships. 2nd ed. John Wiley & Sons, New York.
- Blake, G.R., and K.H. Hartge. 1986. Bulk density. p. 363-375. In A. Klute (ed.) *Methods of soil analysis*. Part 1. 2nd ed. Agron. Monogr. 9. ASA and SSSA, Madison, WI.
- Bullock, D.S., and D.G. Bullock. 2000. Economic optimality of input application rates in precision farming. *Precis. Agric.* 2:71-101.
- Carter, L.M., J.D. Rhoades, and J.H. Chesson. 1993. Mechanization of soil salinity assessment for mapping. Paper 931557. Proc. ASAE Winter Meet., Chicago, IL. 12-17 Dec. 1993. ASAE, St. Joseph, MI.
- Corwin, D.L., S.R. Kaffka, J.W. Hopmans, Y. Mori, J.W. van Groenigen, C. van Kessel, S.M. Lesch, and J.D. Oster. 2003. Assessment and field-scale mapping of soil quality properties of a saline-sodic soil. *Geoderma* (in press).
- Corwin, D.L., and S.M. Lesch. 2003. Application of soil electrical conductivity to precision agriculture: Theory, principles, and guidelines. *Agron. J.* 95:(in press).
- Cressie, N.A. 1993. *Statistics for spatial data*. John Wiley & Sons, New York.
- Engman, E.T. 1999. Remote sensing in hydrology. p. 165-177. In D.L. Corwin, K. Loague, and T.R. Ellsworth (ed.) *Assessment of non-point source pollution in the vadose zone*. Geophysical Monogr. 108. Am. Geophysical Union, Washington, DC.
- Gee, G.W., and J.W. Bauder. 1986. Particle-size analysis. p. 383-411. In A. Klute (ed.) *Methods of soil analysis*. Part 1. 2nd ed. Agron. Monogr. 9. ASA and SSSA, Madison, WI.
- Gotway, C.A., R.B. Ferguson, G.W. Hergert, and T.A. Peterson. 1996. Comparison of kriging and inverse-distance methods for mapping soil parameters. *Soil Sci. Soc. Am. J.* 60:1237-1247.

- Hanks, J., and J.T. Ritchie (ed.). 1991. Modeling plant and soil systems. Agron. Monogr. 31. ASA, CSSA, and SSSA, Madison, WI.
- Harradine, F.F. 1950. Soils of Western Fresno County California. Univ. of California, Berkeley.
- Jaynes, D.B., T.S. Colvin, and J. Ambuel. 1993. Soil type and crop yield determinations from ground conductivity surveys. ASAE Paper 933552. ASAE, St. Joseph, MI.
- Jaynes, D.B., T.S. Colvin, and J. Ambuel. 1995. Yield mapping by electromagnetic induction. p. 383-394. *In* P.C. Robert et al. (ed.) Site-specific management for agricultural systems. ASA, CSSA, and SSSA, Madison, WI.
- Kitchen, N.R., K.A. Sudduth, and S.T. Drummond. 1996. Mapping of sand deposition from 1993 midwest floods with electromagnetic induction measurements. *J. Soil Water Conserv.* 51:336-340.
- Kitchen, N.R., K.A. Sudduth, and S.T. Drummond. 1999. Soil electrical conductivity as a crop productivity measure for claypan soils. *J. Prod. Agric.* 12:607-617.
- Kravchenko, A., and D.G. Bullock. 1999. A comparative study of interpolation methods for mapping soil properties. *Agron. J.* 91:393-400.
- Larson, W.E., and P.C. Robert. 1991. Farming by soil. p. 103-112. *In* R. Lal and F.J. Pierce (ed.) Soil management for sustainability. Soil and Water Conserv. Soc., Ankeny, IA.
- Laslett, G.M., A.B. McBratney, P.J. Pahl, and M.F. Hutchinson. 1987. Comparison of several spatial prediction methods for soil pH. *J. Soil Sci.* 38:325-341.
- Leenaers, H., J.P. Okx, and P.A. Burrough. 1990. Comparison of spatial prediction methods for mapping floodplain soil pollution. *Catena* 17:535-550.
- Lesch, S.M., J.D. Rhoades, and D.L. Corwin. 2000. ESAP-95 Version 2.01R: User manual and tutorial guide. Res. Rep. 146. USDA-ARS George E. Brown, Jr., Salinity Lab., Riverside, CA.
- Lesch, S.M., D.J. Strauss, and J.D. Rhoades. 1995a. Spatial prediction of soil salinity using electromagnetic induction techniques: I. Statistical prediction models: A comparison of multiple linear regression and cokriging. *Water Resour. Res.* 31:373-386.
- Lesch, S.M., D.J. Strauss, and J.D. Rhoades. 1995b. Spatial prediction of soil salinity using electromagnetic induction techniques: II. An efficient spatial sampling algorithm suitable for multiple linear regression model identification and estimation. *Water Resour. Res.* 31:387-398.
- Littell, R.C., G.A. Milliken, W.W. Stroup, and R.D. Wolfinger. 1996. SAS systems for mixed models. SAS Inst., Cary, NC.
- Long, D.S. 1998. Spatial autoregression modeling of site-specific wheat yield. *Geoderma* 85:181-197.
- Maas, E.V. 1984. Salt tolerance of plants. p. 57-75. *In* B.R. Christie (ed.) Handbook of plant science. CRC Press, Cleveland, OH.
- Maas, E.V., and G.J. Hoffman. 1977. Crop salt tolerance—current assessment. *J. Irrig. Drain. Div., Am. Soc. Civ. Eng.* 103(IR2):115-134.
- McNeil, J.D. 1992. Rapid, accurate mapping of soil salinity by electromagnetic ground conductivity meters. p. 201-229. *In* G.C. Topp, W.D. Reynolds, and R.E. Green (ed.) Advances in measurement of soil physical properties: Bringing theory into practice. SSSA Spec. Publ. 30. SSSA, Madison, WI.
- Page, A.L., A.C. Chang, and D.C. Adriano. 1990. Deficiencies and toxicities of trace elements. p. 138-160. *In* K.K. Tanji (ed.) Agricultural salinity assessment and management. ASCE, New York.
- Page, A.L., R.H. Miller, and D.R. Kenney (ed.). 1982. Methods of soil analysis. Part 2. 2nd ed. Agron. Monogr. 9. ASA and SSSA, Madison, WI.
- Rhoades, J.D. 1992a. Instrumental field methods of salinity appraisal. p. 231-248. *In* G.C. Topp, W.D. Reynolds, and R.E. Green (ed.) Advances in measurement of soil physical properties: Bringing theory into practice. SSSA Spec. Publ. 30. SSSA, Madison, WI.
- Rhoades, J.D. 1992b. Recent advances in the methodology for measuring and mapping soil salinity. Proc. Intl. Symp. Strategies for Utilizing Salt-Affected Lands, ISSS Meet., Bangkok, Thailand. 17-25 Feb. 1992. ISSS, Vienna, Austria.
- Rhoades, J.D., F. Chanduvi, and S. Lesch. 1999a. Soil salinity assessment: Methods and interpretation of electrical conductivity measurements. FAO Rep. 57. FAO, Rome.
- Rhoades, J.D., D.L. Corwin, and S.M. Lesch. 1999b. Geospatial measurements of soil electrical conductivity to assess soil salinity and diffuse salt loading from irrigation. p. 197-215. *In* D.L. Corwin, K. Loague, and T.R. Ellsworth (ed.) Assessment of non-point source pollution in the vadose zone. Geophysical Monogr. 108. Am. Geophysical Union, Washington, DC.
- SAS Institute. 1999. SAS software, version 8.2. SAS Inst., Cary, NC.
- Shapiro, S.S., and M.B. Wilk. 1965. An analysis of variance test for normality (complete samples). *Biometrika* 52:591-611.
- Suarez, D.L., J.D. Rhoades, R. Lavado, and C.M. Grieve. 1984. Effect of pH on saturated hydraulic conductivity and soil dispersion. *Soil Sci. Soc. Am. J.* 48:50-55.
- Sudduth, K.A., N.R. Kitchen, D.F. Hughes, and S.T. Drummond. 1995. Electromagnetic induction sensing as an indicator of productivity on claypan soils. p. 671-681. *In* P.C. Robert et al. (ed.) Site-specific management for agricultural systems. ASA, CSSA, and SSSA, Madison, WI.
- Tanji, K.K. (ed.). 1996. Agricultural salinity assessment and management. ASCE, New York.
- Thornley, J.H.M., and I.R. Johnson. 1990. Plant and crop modeling—a mathematical approach to plant and crop physiology. Clarendon Press, Oxford, UK.
- van Schilfgaarde, J. 1999. Is precision agriculture sustainable? *Am. J. Altern. Agric.* 14(1):43-46.
- Warrick, A.W., R. Zhang, M.K. El-Harris, and D.E. Myers. 1988. Direct comparisons between kriging and other interpolators. p. 505-510. *In* P.J. Wierenga and D. Bachelet (ed.) Validation of flow and transport models for the unsaturated zone. Proc. Int. Conf. and Workshop, Ruidoso, NM. 23-26 May 1988. New Mexico State Univ., Las Cruces.
- Weber, D.D., and E.J. Englund. 1992. Evaluation and comparison of spatial interpolators. *Math. Geol.* 24:381-391.
- Wollenhaupt, N.C., R.P. Wolkowski, and M.K. Clayton. 1994. Mapping soil test phosphorus and potassium for variable-rate fertilizer application. *J. Prod. Agric.* 7:441-448.